Peertechz

CLINICAL GROUP

INTERNATIONAL JOURNAL OF
Radiology and Radiation Oncology

ISSN: 2640-7566 DOI: https://dx.doi.org/10.17352/ijrro

Ruifeng Wang[1,2], Xiaoyi Duan[1], Cong Shen[1], Dong Han[2], Junchao Ma[2], Hulin Wu[2], Xiaotong Xu[2], tao Qin[2], Qiuju Fan[2], Zhaoguo Zhang[2], Weihua Shi[2] and Youmin Guo[1]*

[1]Department of Medical Image, The First Affiliated Hospital of Xi'an Jiaotong University, Xi'an, 710061, P.R. China

[2]Department of Medical Image, The Affiliated Hospital of Shanxi University of Chinese Medicine, Shananxi, 712000, P.R. China

Received: 05 March, 2018
Accepted: 09 April, 2018
Published: 10 April, 2018

***Corresponding author:** Youmin Guo, Department of Medical Image, The First Affiliated Hospital of Xi'an Jiaotong University, No.277 Yanta West Road, Xi'an, Shananxi, 710061, P.R. China, Tel: +(86)-29-85324741; Fax: +(86)-29-85324743; E-mail: guoyoumin163@sina.com

Keywords: Bone; Pelvis; SPECT/CT; SUV

https://www.peertechz.com

Research Article

A retrospective study of SPECT/CT scans using SUV measurement of the normal pelvis with Tc-99m methylene diphosphonate

Abstract

Objective: This study aimed to perform the quantitative measurement based on the standardized uptake value (SUV) of Tc-99m methylene diphosphonate (MDP) in normal pelvis using a single-photon emission tomography (SPECT)/computed tomography (CT) scanner.

Material and Methods: This retrospective study was performed on 31 patients with cancer undergoing bone SPECT/CT scans with ^{99m}Tc-MDP between August and December 2016. SUV_{max} and SUV_{mean} of the normal pelvis were calculated based on the body weight. SUV_{max} and SUV_{mean} of the bilateral anterior superior iliac spine, posterior superior iliac spine, facies auricularis ossis ilii, ischial tuberosity, and sacrum were calculated. Further, the correlation of SUV_{max} and SUV_{mean} of all parts of the pelvis with weight, height, and CT was studied.

Results: The data for 31 patients (20 women and 11 men; mean age 58.97± 9.12 years; age range 37–87 years) were acquired. SUV_{max} and SUV_{mean} changed from 1.65 ± 0.40 to 3.8 ± 1 and from 1.15 ± 0.25 to 2.07 ± 0.58, respectively. The coefficient of variation of SUV_{max} and SUV_{mean} ranged from 0.22 to 0.31. SUV_{max} and SUV_{mean} had no statistically significant difference between men and women. SUV_{max} and SUV_{mean} showed no significant correlation with weight and height. Part of SUV_{max} and SUV_{mean} showed a significant correlation with CT. However, SUV_{max} and SUV_{mean} of bilateral ischial tuberosity showed a significant correlation with CT values.

Conclusions: SUVs of the normal pelvis showed a relatively large variability. As a quantitative imaging biomarker, SUVs might require standardization with adequate reference data for the participant to minimize variability.

Introduction

Currently the most commonly used tracer for imaging the skeleton in conventional nuclear medicine is technetium-99m-labeled methylene diphosphonate (^{99m}Tc-MDP) bone scintigraphy, which is a cost-effective and useful tool and has variable diagnostic sensitivity with comparatively low specificity [1]. Bone scintigraphy is the standard of reference in bone metastases in cancer patients. The most common primary sites for bone metastases are lung, breast, prostate, kidney, and thyroid. The axial skeleton and the pelvis are the most common metastasis locations [2-7]. ^{99m}Tc-MDP and hydroxymethylene diphosphonate have been widely used for bone scintigraphy [8]. Single-photon emission tomography (SPECT)/computed tomography (CT) scanner provides fusion images of CT and SPECT and also produces attenuation correction maps and directly correlated bone scan findings with anatomic structures [9,10].

Quantitative measurements have become vastly important with advances in molecular imaging. Sullivan developed various quantitative imaging biomarkers (QIBs). However, few of these QIBs are used routinely in clinical trials or clinical care [11,12]. Quantitative analyses have been performed for bone scans of vertebrae using the standardized uptake value (SUV) as QIB of SPECT/CT scans with ^{99m}Tc-MDP [8,13]. SUV is defined as the tissue concentration of tracer as measured by a positron emission tomography (PET) scanner divided by the activity concentration injected divided usually by body weight [8,14,15]. The uptake value is represented by pixel or voxel intensity value in the region of interest (ROI) of the image, which is then converted into the activity concentration. SUVs

Citation: Wang R, Duan X, Shen C, Han D, Ma J, et al. (2018) A retrospective study of SPECT/CT scans using SUV measurement of the normal pelvis with Tc-99m methylene diphosphonate. Int J Radiol Radiat Oncol 4(1): 003-008. DOI: http://dx.doi.org/10.17352/ijrro.000027

represent tissue activity within an ROI corrected for injected activity and body weight [16].

The pelvis in the most common localization after spine in bone metastasis [3]. The detection of occult bone metastases is a key factor in determining the management of patients with cancer, which can greatly alter patient management [13]. ^{99m}Tc-MDP bone scans showed hot spots in the lower lumbar region of the spine and/or the pelvic bone [17], it was difficult to identify bone metastases in the early stages by visual evaluation. Thus, it is important to address the question of quantitative evaluation of hot spots in the pelvic bone. However, few reports have been published on SUV measurement as QIB in bone imaging using SPECT/CT scans with ^{99m}Tc-MDP. The primary aim of this study was to report the SUV of the normal pelvis with absolute values, deviation, and variability. Furthermore, the correlations of SUV_{max}, SUV_{mean} with height, weight, and CT were determined.

Methods

Patients

In this study, all patients were examined for staging malignancy, such as prostate cancer, pancreatic cancer, breast cancer, colon cancer, renal cancer, lung cancer, gastric cancer, and ovarian cancer. The data of patients with normal pelvis who underwent bone scans were retrospectively analyzed. Patient data analysis was carried out with permission from the Ethics Committee of the Affiliated Hospital of Shaanxi University of Chinese Medicine. Data were required for a group of 31 patients (20 women and 11 men) undergoing Tc-99m MDP (Atomic High-tech Co. Ltd, Beijing, China) bone SPECT/CT between August and December 2016.

The patients were included based on the following criteria: (1) access to data on measured injection activity, time of measurement, and time of injection; (2) access to patient's weight and height information; (3) SPECT/CT scans for pelvis; and (4) absence of diffuse bone metastases, ankylosing spondylitis, metabolic bone disease, and osteoarthritis.

Data acquisition and reconstruction

The measurements of system sensitivity, which vary depending on the radionuclide, thickness of the scintillation crystal, collimator, and pulse height analyzer energy windows used [18]. The Symbia T16 (CT with a maximum of 16 slice acquisitions per rotation, Siemens Healthcare, Molecular Imaging, IL, USA) system was used for SPECT/CT scans. The SPECT/CT scans with 3/8 inch NaI(Tl) detector and low-energy, high resolution collimator were acquired, a 128 × 128 matrix of 4.8-mm pixel size, and a total of 450 s/rotation in a continuous-rotation mode. The pulse height analyzer energy windows were 140Kev±15%. Subsequent to the SPECT acquisition, a low-dose CT scan was acquired with 130 kV and 15 ref mAs using adaptive dose modulation (CARE Dose 4D; Siemens Healthcare Molecular Imaging, IL, USA). The CT data were generated with a 1.5-mm slice thickness using a smooth reconstruction B70s kernel. SPECT reconstruction was performed using filtered back-projection, and attenuation correction was based on attenuation maps derived from the CT data filtered with the B70s kernel.

The patient's clinical data was acquired from the hospital's HIS database.

Data analysis

The WBS and SPECT/CT images were independently interpreted by two experienced nuclear medicine physicians and a diagnostic radiologist. In cases of discrepancy, the consensus was obtained by a joint reading. From the pelvis scanned, SUVs of 31 pelves were calculated for analyses based on the previously defined criteria [18]. The delineation of the volumes of interest (VOIs) was performed using a newly released software "Dynamic analysis" provided by Beijing Dynamic Analysis Medical Information Technology Co., Ltd. (Beijing, China), which reported the statistics for the SUV_{max} and SUV_{mean}. The VOIs were plotted by manually adjusting the boundary of VOIs of SPECT and the boundary of the spongy bone of pelvis on CT images.

The SPECT/CT system was calibrated with a uniform phantom, which provided a volume sensitivity factor and was specific to the camera type, collimator type, and the window energy settings used. The patient's reconstructed values were then normalized with volume sensitivity. All data were decay-corrected to the time of injection to control fluctuations at the start time of the acquisition. Final values of quantitative tracer concentrations were thus defined with respect to injection time.

Statistical analyses

The degree of dispersion of SUV_{max} and SUV_{mean} of the normal pelvis were evaluated using the coefficient of variation (CV). The data was analyzed using normal distribution test. Only the continuous variables that satisfied the normal distribution were tested using *t* test. Differences in SUVs between male and female participants were tested using a paired two-sample *t* test assuming equal variation. The relationships of SUVs with weight, height, and CT values were evaluated with a Pearson's correlation analysis. *P* values less than 0.05 indicated significant differences. All analyses were computed using SPSS16.0 (IBM, USA).

Results

In this study, 31 patients were examined for staging malignancy, including prostate cancer, pancreatic cancer, breast cancer, colon cancer, renal cancer, lung cancer, gastric cancer, and ovarian cancer. The data for a group of 31 patients undergoing Tc-99m MDP bone SPECT/CT were collected. The injected activity of ^{99m}Tc-MDP was 749.6 ± 83.25 MBq (20.26 ± 2.25 mCi) corresponding to 8.51–17.76 MBq/kg (0.34 ± 0.07 mCi/kg). Planar and SPECT/CT images were acquired about 3–4 h after intravenous injection. The VOIs of bilateral anterior superior iliac spine, posterior superior iliac spine, facies auricularis ossis ilii, ischial tuberosity, and sacrum were plotted by manually adjusting the boundary of SPECT and the boundary of the spongy bone of pelvis on CT images (Figure 1).

Citation: Wang R, Duan X, Shen C, Han D, Ma J, et al. (2018) A retrospective study of SPECT/CT scans using SUV measurement of the normal pelvis with Tc-99m methylene diphosphonate. Int J Radiol Radiat Oncol 4(1): 003-008. DOI: http://dx.doi.org/10.17352/ijrro.000027

SUV_{max} and SUV_{mean}

SUV_{max} and SUV_{mean} of the normal pelvis were calculated based on body weight. SUVs showed a wide range of values. The values of SUV_{max} and SUV_{mean}, and the CV of SUV_{max} and SUV_{mean} are shown in figure 2 and table 1.

psis-l represents left posterior superior iliac spine, asip-l represents left anterior superior iliac spine; asip-R represents right anterior superior iliac spine; psis-R represents right posterior superior iliac spine; faoi-L represents left facies auricularis ossis ilii; faoi-R represents left facies auricularis ossis ilii; it-L represents left ischial tuberosity; and it-R represents right ischial tuberosity. Values shown are mean ± SD.

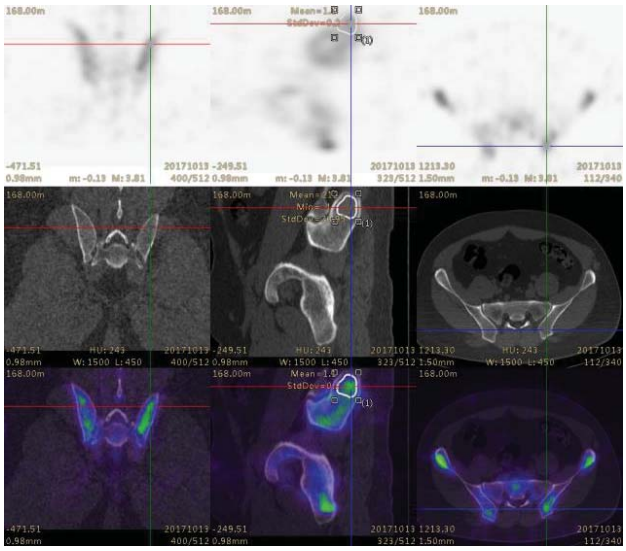

Figure 1: Transaxial, saggital and coronal images of a patient's SPECT/CT fused data of pevis.

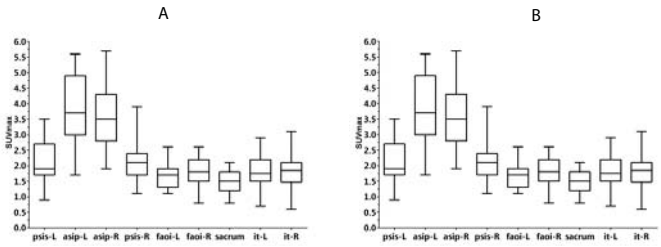

Figure 2: (A and B) Box-and-whisker plots of SUV_{max} and SUV_{mean} showing a quantitative distribution of pelvis statistics.

Among the 31 normal pelves for which SUVs were calculated, 1 ischial tuberosity of the normal pelvis was excluded for the following statistical analyses because ischial nodules were not included in the scan range of SPECT/CT (Table 1).

SUVamx and SUVmean are normal distribution, and then we do T tests and Pearson's correlation. SUV_{max} and SUV_{mean} of all part of pelvis showed weak and no significant correlation with weight and height (Tables 2,3). On the contrary, SUV_{max} and SUV_{mean} of part of pelvis showed moderate and significant correlation with CT values. SUVmean of left posterior superior iliac spine and SUV_{max} of left anterior superior iliac spine showed a significant correlation with CT (R = 0.412 P = 0.02; R = 0.367, P = 0.04), SUV_{max} and SUV_{mean} of facies auricularis ossis ilii and bilateral ischial tuberosity showed a significant correlation with CT (R = 0.399 P = 0.03, R = 0.545 P < 0.01; R = 0.498 P = 0.01, R = 0.692 P < 0.01; R = 0.594 P < 0.01, R = 0.558 P < 0.01). Furthermore, SUVmax of right of facies auricularis ossis ilii showed a significant correlation with CT. SUV_{max} and SUV_{mean} of other parts of pelvis showed weak and no significant correlation with CT values (Table 4).

psis-l represents left posterior superior iliac spine; asip-l represents left anterior superior iliac spine; asip-R represents right anterior superior iliac spine; psis-R represents right posterior superior iliac spine; faoi-L represents left facies auricularis ossis ilii; faoi-R represents left facies auricularis ossis ilii; it-L represents left ischial tuberosity; and it-R represents right ischial tuberosity. Values shown are mean ± SD (*P < 0.05; ** P < 0.01).

psis-l represents left posterior superior iliac spine; asip-l represents left anterior superior iliac spine; asip-R represents right anterior superior iliac spine; psis-R represents right posterior superior iliac spine; faoi-L represent left facies auricularis ossis ilii; faoi-R represents left facies auricularis ossis ilii; it-L represents left ischial tuberosity; and it-R represent right ischial tuberosity. Values shown are mean ± SD (*P < 0.05; ** P < 0.01).

psis-l represents left posterior superior iliac spine; asip-l represents left anterior superior iliac spine; asip-R represents right anterior superior iliac spine; psis-R represents right

Table 1: SPECT/CT scans using the SUV measurement of normal pelvis Correlation with weight, height, and CT values

Locations	CT attenuation values			SUV_{max}			SUV_{mean}		
	Mean	SD	CV	Mean	SD	CV	Mean	SD	CV
psis-L*(n=31)*	106.00	45.65	0.43	2.11	0.65	0.31	1.52	0.48	0.31
asip-L*(n=31)*	200.32	56.24	0.28	3.80	1.00	0.26	2.07	0.58	0.28
asip-R*(n=31)*	196.06	63.10	0.32	3.63	1.01	0.28	1.82	0.63	0.34
psis-R*(n=31)*	115.94	48.35	0.42	2.10	0.64	0.31	1.52	0.45	0.29
faoi-L*(n=31)*	159.84	63.08	0.39	1.65	0.40	0.24	1.22	0.31	0.25
faoi-R*(n=31)*	171.48	66.72	0.39	1.77	0.45	0.25	1.30	0.37	0.29
sacrum*(n=31)*	164.77	55.81	0.34	1.50	0.33	0.22	1.15	0.25	0.22
it-L*(n=30*)*	178.73	71.36	0.40	1.83	0.57	0.31	1.20	0.32	0.27
it-R*(n=30*)*	186.43	77.76	0.42	1.79	0.55	0.31	1.22	0.35	0.29

Citation: Wang R, Duan X, Shen C, Han D, Ma J, et al. (2018) A retrospective study of SPECT/CT scans using SUV measurement of the normal pelvis with Tc-99m methylene diphosphonate. Int J Radiol Radiat Oncol 4(1): 003-008. DOI: http://dx.doi.org/10.17352/ijrro.000027

posterior superior iliac spine; faoi-L represent left facies auricularis ossis ilii; faoi-R represents left facies auricularis ossis ilii; it-L represents left ischial tuberosity; and it-R represent right ischial tuberosity. Values shown are mean ± SD (*$P < 0.05$; ** $P < 0.01$).

Differences between male and female participants

In this study, the average age (58.97 ± 9.12) of male and female participants was 62.55 ± 7.88 and 57.00 ± 9.34, respectively. No significant differences were found between male and female participants with regard to the SUVmax and SUVmean (Figure 3).

psis-l represents left posterior superior iliac spine; asip-l represents left anterior superior iliac spine; asip-R represents right anterior superior iliac spine; psis-R represents right posterior superior iliac spine; faoi-L represents left facies auricularis ossis ilii; faoi-R represents left facies auricularis ossis ilii; it-L represents left ischial tuberosity; and it-R represents right ischial tuberosity. Values shown are mean ± SD (all $P > 0.05$; error bar is SD).

Discussion

SPECT/CT scanners have given renewed impetus to produce quantitative SPECT data. The CT data complement the SPECT data, which can be used to correct for photons that have been Compton-scattered or attenuated within the body. Also, algorithms for image reconstruction and sophisticated compensation techniques to correct for photon attenuation and scattering have made quantitative SPECT viable in a manner similar to quantitative PET (i.e., kBqcm^{-3}, SUV) [18,19]. SPECT has some advantages over PET: the physical half-lives for many SPECT radionuclides are generally longer and more aligned with the biologic half-lives of physiologic processes of interest [18]. Quantitative measurements have become vastly important with advances in molecular imaging. SUV might be useful as an appropriate quantitative biomarker (quantitative imaging biomarkers) in bone SPECT/CT imaging and was thought to be useful for the evaluating the activities of bone lesions and the response to therapy [2].

SUV_{max} and SUV_{mean} of each part of the normal pelvis were calculated and evaluated, which had the narrow spread. The mean ± standard deviation (SD) of SUV_{max} and SUV_{mean} changed from 1.65 ± 0.40 to 3.8 ± 1 and from 1.15 ± 0.25 to 2.07 ± 0.58, respectively. The values of SUV_{max} and SUV_{mean} of the normal pelvis were lower than those of the vertebral body [8]. The CV of SUV_{max} and SUV_{mean} ranged from 0.22 to 0.31. Cachovan et al., reported a significant negative correlation between age and both SUVbw and SUVlbw of Tc-^{99m} diphosphono-propanedicarboxylic acid (DPD) SPECT [20]. The present study showed that the age span of the patients ranged from 37 to 87 years. That was the reason why CV of SUV_{max} and SUV_{mean} was large.

The results demonstrated that SUV_{max} and SUV_{mean} of all parts of the normal pelvis did not show a significant correlation with height and weight (Tables 3,4). However, Tomohiro et al. reported that the SUVs of normal vertebrae showed moderate and significant correlation with the height of the participants [8]. The VOI of vertebrae were seated over cancellous bone

Table 2: Correlation coefficients between SUVs and weight

SUV_{max}	*R*	*P*	SUV_{mean}	*R*	*P*
psis-L	−0.152	0.41	psis-L	−0.116	0.53
asip-L	0.013	0.94	asip-L	−0.158	0.40
asip-R	−0.060	0.75	asip-R	−0.234	0.21
psis-R	−0.128	0.49	psis-R	−0.176	0.34
faoi-L	0.020	0.92	faoi-L	0.035	0.85
faoi-R	−0.095	0.61	faoi-R	−0.049	0.79
sacrum	−0.222	0.23	sacrum	−0.220	0.23
it-L	0.166	0.38	it-L	0.273	0.14
it-R	0.155	0.41	it-R	0.297	0.11

Table 3: Correlation coefficients between SUVs and height

SUV_{max}	*R*	*P*	SUV_{mean}	*R*	*P*
psis-L	−0.043	0.82	psis-L	−0.063	0.74
asip-L	0.052	0.78	asip-L	0.019	0.92
asip-R	0.210	0.26	asip-R	0.024	0.90
psis-R	0.038	0.84	psis-R	−0.038	0.84
faoi-L	−0.025	0.89	faoi-L	−0.031	0.87
faoi-R	−0.164	0.38	faoi-R	−0.134	0.47
sacrum	−0.170	0.36	sacrum	−0.097	0.60
it-L	0.010	0.96	it-L	−0.202	0.28
it-R	−0.054	0.78	it-R	−0.034	0.86

Table 4: Correlation coefficients between SUVs and CT values

	SUV_{max}		SUV_{mean}	
CT	*R*	*P*	*R*	*P*
psis-L	0.273	0.14	0.412	0.02*
asip-L	0.367	0.04*	0.257	0.16
asip-R	0.307	0.09	0.129	0.49
psis-R	0.247	0.18	0.306	0.09
faoi-L	0.279	0.13	0.304	0.10
faoi-R	0.399	0.03*	0.545	<0.01**
sacrum	0.269	0.14	0.136	0.46
it-L	0.498	0.01*	0.594	<0.01**
it-R	0.692	<0.01**	0.558	<0.01**

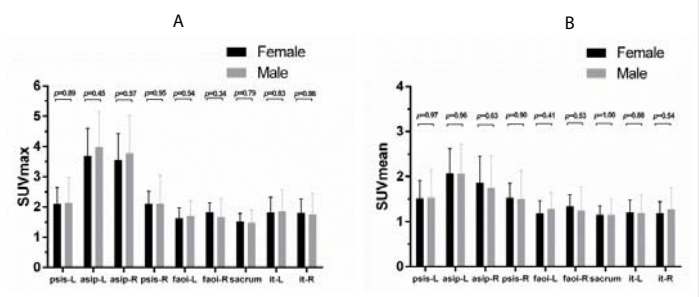

Figure 3: (A and B) SUVs showing no significant differences between male and female participants.

Citation: Wang R, Duan X, Shen C, Han D, Ma J, et al. (2018) A retrospective study of SPECT/CT scans using SUV measurement of the normal pelvis with Tc-99m methylene diphosphonate. Int J Radiol Radiat Oncol 4(1): 003-008. DOI: http://dx.doi.org/10.17352/ijrro.000027

and bone cortex. The increase in physical burden due to a high center of gravity might increase bone density [8]. Of note, in adult males, bone marrow is confined to about 38% of the skeleton axial skeleton that is pelvis [21]. The VOI only covered the cancellous bone of the pelvis. And not all parts of pelvis participated in bearing the load of body weight. The changes in SUV_{max} and SUV_{mean} reflected bone marrow metabolism. Therefore, no significant correlation was found between the SUVs and height and body weight of the participants.

In Tomohiro study, the mean age of male participants was about 5 years higher than that of female participants. SUVs of the males were higher than those of females, and the difference was significant [8]. The result of the present study showed that the mean age of male participants was about 5 years higher than that of female participants, and the difference in SUVs between males and females was not significant. The reason for the difference in SUVs of the normal pelvis between males and females was the difference in participants.

The results showed that the correlation of bilateral SUV_{max} and SUV_{mean} of the pelvis with CT was asymmetrical, SUV_{max} and SUV_{mean} of the right of facies auricularis ossis ilii showed a significant correlation with CT. However, SUV_{max} and SUV_{mean} of left of facies auricularis ossis ilii and right posterior superior iliac spine showed no significant correlation with CT. The left and right outcomes were different from each other because forces on the left and right sides of the posterior superior iliac spine were different due to the impact of handedness on the different characteristics and advantages between left- and right-handers [22]. Bone density was correlated with the physical and structural density of hydroxyapatite in the bones as well as with HU determined using CT [20]. The results showed that SUV_{max} and SUV_{mean} of ischial tuberosity were correlated with HU. The ischial tuberosities were the stress point of a person's weight when the person sat down [23]. The ^{99m}Tc-MDP bound to the calcium-rich tissue and the mineral phase of bone hydroxyapatite [24]. Michal Cachovan's results showed a strong correlation of tracer activity concentration with bone density expressed in HU [20]. Furthermore, the spongy bone of ischial tuberosities comprised trabecular bone interspersed with marrow and rich vasculature filled with marrow [21]. The cortical bone of anterior superior iliac spine was the attachment point of ligament [25]. The SUV_{max} was not affected by degenerative or malignant diseases and did not burden the body weight. The ^{99m}Tc-MDP was taken up in the spongy bone tissue interspersed with marrow.

SPECT/CT readily achieves accuracy for ^{99m}Tc to within ±10% of the known concentration of the radiotracer *in vivo*. Quantification with other radionuclides has also been introduced. It is beneficial in some situations of longer radionuclide half-lives. It may better suit the biologic process under examination and the ability to perform multitracer studies using pulse height spectroscopy to separate different radiolabels.

The main limitation of the present study was its small sample size. Also, it was a retrospective study, and repeated measurements of intraindividual variability could not be performed. Using lean mass or body surface area to normalize the data might help reduce data variability. Modern SPECT systems use iterative reconstruction algorithms such as ordered subsets expectation maximization (OSEM), rather than FBP, We compare the effect of FBP and iterative reconstruction method on SUVs in the future. The diagnostic accuracy of range in the present study needs further verification.

Conclusions

SUVs of the normal pelvis showed a relatively large variability. As a quantitative imaging biomarker, SUVs might require standardization with adequate reference data for the participants to minimize variability.

Acknowledgments

This work was supported by funding from the Public Science and Technology Research Funds of China (No. 201402013).

References

1. Ak I, Sivrikoz MC, Entok E, Vardareli E (2010) Discordant findings in patients with non-small-cell lung cancer: absolutely normal bone scans versus disseminated bone metastases on positron-emission tomography/computed tomography. Eur J Cardiothorac Surg 37: 792-796. Link: https://goo.gl/FXHQRh

2. Doddala SM, Suryadevara A, Chinta SK, Madisetty AL (2016) Incidence and pattern of bone metastases at presentation in Indian carcinoma breast patients. Indian J Cancer 53: 360-362. Link: https://goo.gl/5XU5Zj

3. Spinelli MS, Ziranu A, Piccioli A, Maccauro G (2016) Surgical treatment of acetabular metastasis. Eur Rev Med Pharmacol Sci 20: 3005-3010. Link: https://goo.gl/H4wRov

4. Tsuya A, Kurata T, Tamura K, Fukuoka M (2007) Skeletal metastases in non-small cell lung cancer: a retrospective study. Lung Cancer 57: 229-232. Link: https://goo.gl/7Ksf5U

5. Stephen C, Jacobs (1983) Spread of prostatic cancer to bone. Urology 21: 337-344. Link: https://goo.gl/P3WtSF

6. Chen XY, Lan M, Zhou Y, Chen WZ, Hu D, et al. (2017) Risk factors for bone metastasis from renal cell cancer. J Bone Oncol 9: 29-33. Link: https://goo.gl/PzdyRu

7. Lin JD, Hsueh C, Chao TC (2015) Long-Term Follow-Up of the Therapeutic Outcomes for Papillary Thyroid Carcinoma With Distant Metastasis. Medicine (Baltimore) 94: e1063. Link: https://goo.gl/oUhFDE

8. Kaneta T, Ogawa M, Daisaki H, Nawata S, Yoshida K, et al. (2016) SUV measurement of normal vertebrae using SPECT/CT with Tc-^{99m} methylene diphosphonate. Am J Nucl Med Mol Imaging 6: 262-268. Link: https://goo.gl/CDWRAV

9. Keyes JW Jr (1995) SUV: standard uptake or silly useless value? J Nucl Med 36: 1836-1839. Link: https://goo.gl/nq1j9e

10. Meikle SR, Hutton BF, Bailey DL (1994) A transmission-dependent method for scatter correction in SPECT. J Nucl Med 35: 360-367. Link: https://goo.gl/ichFwc

11. Sullivan DC, Obuchowski NA, Kessler LG, Raunig DL, Gatsonis C, et al. (2015) Metrology Standards for Quantitative Imaging Biomarkers. Radiology 277: 813-825. Link: https://goo.gl/7DJKDY

12. Nakamura Y, Tomiguchi S, Tanaka M (2015) Reliability and advantages of using non-uniform Chang's attenuation correction method using a CT-based attenuation coefficient map in (^{99m})Tc-GSA SPECT/CT hepatic imaging. EJNMMI Phys 2: 17. Link: https://goo.gl/1XhiKP

Citation: Wang R, Duan X, Shen C, Han D, Ma J, et al. (2018) A retrospective study of SPECT/CT scans using SUV measurement of the normal pelvis with Tc-99m methylene diphosphonate. Int J Radiol Radiat Oncol 4(1): 003-008. DOI: http://dx.doi.org/10.17352/ijrro.000027

13. Gerety EL, Lawrence EM, Wason J, Yan H, Hilborne S, et al. (2015) Prospective study evaluating the relative sensitivity of 18F-NaF PET/CT for detecting skeletal metastases from renal cell carcinoma in comparison to multidetector CT and ^{99m}Tc-MDP bone scintigraphy, using an adaptive trial design. Ann Oncol 26: 2113-2118. Link: https://goo.gl/GhtMNV

14. Huang SC (2000) Anatomy of SUV. Standardized uptake value. Nucl Med Biol 27: 643-646. Link: https://goo.gl/u2zkkM

15. Thie JA (2004) Understanding the standardized uptake value, its methods, and implications for usage. J Nucl Med 45: 1431-1434. Link: https://goo.gl/vHTP1k

16. Win AZ, Aparici CM (2014) Normal SUV values measured from NaF18- PET/CT bone scan studies. PLoS One 9: e108429. Link: https://goo.gl/kuQ3uP

17. Otsuka N, Fukunaga M, Morita R, Sone T, Yoneda M, et al. (1985) [The usefulness of bone marrow scintigraphy in the detection of bone metastasis from prostatic cancer]. Kaku Igaku 22: 169-176. Link: https://goo.gl/zxyHCi

18. Bailey DL, Willowson KP (2013) An evidence-based review of quantitative SPECT imaging and potential clinical applications. J Nucl Med 54: 83-89. Link: https://goo.gl/yKeAoi

19. Mittal BR, Sood A, Shukla J, Vatsa R, Bhusari P, et al. (2018) ^{99m}Tc-TRODAT-1 SPECT/CT imaging as a complementary biomarker in the diagnosis of parkinsonian syndromes. Nucl Med Commun 39: 312-318. Link: https://goo.gl/2NWHSY

20. Cachovan M, Vija AH, Hornegger J, Kuwert T (2013) Quantification of ^{99m}Tc-DPD concentration in the lumbar spine with SPECT/CT. EJNMMI Res 3: 45. Link: https://goo.gl/8fyfcG

21. Bussard KM, Gay CV, Mastro AM (2008) The bone microenvironment in metastasis; what is special about bone? Cancer Metastasis Rev 27: 41-55. Link: https://goo.gl/eyAoed

22. Gumustekin K, Akar S, Dane S, Yildirim M, Seven B, et al. (2004) Handedness and bilateral femoral bone densities in men and women. Int J Neurosci 114: 1533-1547. Link: https://goo.gl/hXcpXb

23. Hamanami K, Tokuhiro A, Inoue H (2004) Finding the optimal setting of inflated air pressure for a multi-cell air cushion for wheelchair patients with spinal cord injury. Acta Med Okayama 58: 37-44. Link: https://goo.gl/wmxh29

24. Schwartz Z, Shani J, Soskolne WA, Touma H, Amir D, et al. (1993) Uptake and biodistribution of technetium-^{99m}-MD32P during rat tibial bone repair. J Nucl Med 34: 104-108. Link: https://goo.gl/3zFsGQ

25. Rudin D, Manestar M, Ullrich O, Erhardt J, Grob K (2016) The Anatomical Course of the Lateral Femoral Cutaneous Nerve with Special Attention to the Anterior Approach to the Hip Joint. J Bone Joint Surg Am 98: 561-567. Link: https://goo.gl/vUxD3D

Citation: Wang R, Duan X, Shen C, Han D, Ma J, et al. (2018) A retrospective study of SPECT/CT scans using SUV measurement of the normal pelvis with Tc-99m methylene diphosphonate. Int J Radiol Radiat Oncol 4(1): 003-008. DOI: http://dx.doi.org/10.17352/ijrro.000027